Phys. Med. Biol. **49** (2004) 345–354 PII: S0031-9155(04)66623-1

Comparison of FDTD-calculated specific absorption rate in adults and children when using a mobile phone at 900 and 1800 MHz

M Martínez-Búrdalo, A Martín, M Anguiano and R Villar

Consejo Superior de Investigaciones Científicas, Instituto de Física Aplicada, C/Serrano 144, 28006-Madrid, Spain

E-mail: mercedes@iec.csic.es

Received 24 July 2003, in final form 21 November 2003
Published 5 January 2004
Online at stacks.iop.org/PMB/49/345 (DOI: 10.1088/0031-9155/49/2/011)

Abstract

In this paper, the specific absorption rate (SAR) in scaled human head models is analysed to study possible differences between SAR in the heads of adults and children and for assessment of compliance with the international safety guidelines, while using a mobile phone. The finite-difference time-domain method (FDTD) has been used for calculating SAR values for models of both children and adults, at 900 and 1800 MHz. Maximum 1 g averaged SAR ($SAR_{1\,g}$) and maximum 10 g averaged SAR ($SAR_{10\,g}$) have been calculated in adults and scaled head models for comparison and assessment of compliance with ANSI/IEEE and European guidelines. Results show that peak $SAR_{1\,g}$ and peak $SAR_{10\,g}$ all trend downwards with decreasing head size but as head size decreases, the percentage of energy absorbed in the brain increases. So, higher SAR in children's brains can be expected depending on whether the thickness of their skulls and surrounding tissues actually depends on age. The SAR in eyes of different sizes, as a critical organ, has also been studied and very similar distributions for the full size and the scaled models have been obtained. Standard limits can only be exceeded in the unpractical situation where the antenna is located at a very short distance in front of the eye.

(Some figures in this article are in colour only in the electronic version)

1. Introduction

The development of cellular communications and, in particular, the widespread use of mobile phones during the last few years have motivated a great social and scientific concern about possible harmful effects of the electromagnetic radiation from these sources on the user's

health. The most significant parameter when discussing the health risks at these frequencies is the SAR, defined as

$$\mathrm{SAR} = \frac{\sigma |\mathbf{E}|^2}{2\rho},$$

where $\mathbf{E}$ is the maximum value of the internal electric field, σ is the tissue conductivity and ρ is the mass density. The maximum values for the SAR, which must not be exceeded under any circumstance, are specified in radiation protection standards like those of ANSI/IEEE (1992) or the European Commission (1999).

Most of the studies in this sense have focused on predicting the absorbed energy in standard models of an adult human head. Also, almost all the experimental setups to measure the SAR use full scale phantoms based on adult head and body geometries. At present, however, the increasing use of mobile phones by young people has promoted an intensifying public debate about the possible differences between the exposure of adults and children to radiofrequency radiation from mobile phones. For example, the Independent Expert Group on Mobile Phones (IEGMP 2000) recommends that the widespread use of mobile phones by children should be discouraged. One of the reasons for this recommendation is the possible greater energy absorption in the brain tissues of a child's head relative to an adult's head. This topic has been examined in Gandhi and Kang (2001) and larger peak 1 g averaged SARs ($\mathrm{SAR}_{1\ \mathrm{g}}$) are obtained for the body tissues and for the brain with the smaller head model and a deeper penetration of the absorbed energy, for example, for the brain for smaller models has also been obtained. Many other works have studied the exposure of different models of adult heads of different shapes and sizes, comparing inhomogeneous (multi-tissue experimental and numerical phantoms) versus homogeneous models (Hombach *et al* 1996, Okoniewski and Stuchly 1996), and also studying the electromagnetic absorption in head models of adults and children (Gandhi *et al* 1996, Schöborn *et al* 1998), with different conclusions. So, for example, Hombach *et al* (1996) conclude that the spatial peak SAR is scarcely affected by the size and the shape of the human head for electromagnetic sources at a defined (short) distance from the human head and that the overestimation of the averaged spatial peak SAR values with homogeneous models is small when compared to the largest value obtained by the inhomogeneous phantoms, but Gandhi *et al* (1996) have found that both peak one-voxel and $\mathrm{SAR}_{1\ \mathrm{g}}$ are larger for the smaller models of children, particularly at 835 MHz, and also the in-depth penetration of absorbed energy is larger for these smaller models. On the other hand, Schöborn *et al* (1998), by using 0.45-wavelength dipoles as radiators instead of actual mobile telephones, have concluded that there is no difference in the absorption of electromagnetic energy at 900 and 1800 MHz between MRI-based phantoms of adults and children, nor for various linearly scaled adult phantoms and, so, it is sufficient to perform compliance tests with a shell phantom representing the worst-case situation of an adult head, and Wang and Fujiwara (2002, 2003) conclude that the contradictory conclusions drawn by other groups may be due to the different conditions in their numerical peak SAR calculations. Most of these works do not use the same kind of antenna in the simulations, and the head models are not directly equivalent (e.g., in Schöborn *et al* (1998) the scaling is done by reducing the number of voxels by a specified scaling factor and then, in order to preserve the sequence of tissue layers near the feeding point, the cell dimensions are changed along the antenna–head axis according to the scaling factor used previously, while Gandhi *et al* (1996) consider the same number of voxels for all models, and scale down the cell size using the same scaling factor for all three axes). In addition to these discrepancies, a short-term mission entitled 'Mobile Communication and Children' was launched in Europe last year, in the framework of COST 281, and the discussion showed that, in fact, recent research had concentrated on adults and, although it is suggested that simply

downsizing of head structures is not adequate for accounting for children and that analysis of tissue parameters and of the specific anatomical and physiological differences of children compared with adults has to be made, it has concluded that further research on young children has to be carried out (COST 2002). However, although a scaling down of the adult head is not an accurate representation for a child's head, it is not easy to get MRI data directly for children in general (Wang and Fujiwara 2003).

The finite-difference time-domain method (FDTD) is the most widely used technique to compute electromagnetic magnitudes in complex biological tissues and its suitability has been demonstrated (Shlager and Schneider 1995). In this work, high-fidelity computational scaled models have been used to analyse, by means of the FDTD method, the possible differences in absorbed radiation between adults and children exposed to electromagnetic radiations when using a mobile phone, in the frequency bands of 900 and 1800 MHz. Because of the suggested link between temperature rises in the eye and cataract formation (Dimbylow 1993), the energy deposition in the eye, considered as a critical organ (Martínez-Búrdalo *et al* 2001), has also been studied with the emitting antenna located in front of the eye, as a worst case situation, although quite unusual. A brief explanation of the theoretical fundamentals of the technique used and a description of the models are given in section 2. Results comparing the computed SAR values in the different models are shown and discussed in section 3. Finally, conclusions are presented.

2. Fundamentals and models

The FDTD method is a well-known computational technique in which the Maxwell differential equations are discretized using a finite differences scheme implemented in a mesh of cubic cells, named Yee cells (Taflove and Hagness 2000), where the geometries under study are spatially approximated. The cell size must be small enough to permit accurate results at the highest frequency of interest taking into account that the materials present directly affect the wavelength. A lattice of 10 cells per wavelength usually gives accurate results. Once the cell size is selected, the maximum time step is determined by the Courant stability condition. Liao's absorbing boundary conditions are used at the limits of the space under study to avoid undesired reflections (Taflove and Hagness 2000).

In order to study the field penetration into the head and calculate the SAR, we have used the XFDTD program from REMCOM INC, with a realistic 3D human head and shoulders mesh, developed from NMR by REMCOM and the Hershey Medical Center, Hershey, PA. We have considered $309 \times 177 \times 161$ voxels in our model space. The cell dimensions for the adult human head are 0.20 cm in the x (ear to ear) and y directions and 0.25 cm in the z (vertical) direction. To study the dependence of the results on the size of the head, children heads have been modelled by reducing the cell sizes by the factors 0.88 and 0.78 along all three directions. According to the resultant head breadths (144 mm for 0.88 and 128 mm for 0.78), these scaling factors could correspond to 9–10 and 2–3 year old children, respectively (NIST 1977). The same electrical properties and densities have been used, irrespective of the size. These properties are defined in table 1 (Gabriel and Gabriel 1996). A small increase in the dielectric properties for children could be expected if the results of a study with animals (Peyman *et al* 2001) could be extended to humans, but unfortunately there are not yet available data on this subject. The radiation source has been simulated by a vertically polarized, half-wave thin wire dipole at the corresponding working frequency feed at its centre with a series voltage source of 1 V in amplitude. The radiated power is then computed from the feed-point impedance and the feed current and scaled to 250 and 125 mW for 900 and 1800 MHz, respectively, trying to reproduce actual emitting conditions.

(a) (b)

Figure 1. Example of antenna–head geometries: (a) 900 MHz dipole near the ear; (b) 1800 MHz dipole in front of the eye.

Table 1. Densities and electrical properties of the simulated tissues.

		900 MHz		1800 MHz	
Tissue	ρ (kg m^{-3})	ε_r	σ (S m^{-1})	ε_r	σ (S m^{-1})
Skin	1126	39.59	0.693	38.40	0.999
Tendon	1151	46.72	0.951	45.23	1.367
Fat/yellow marrow	943	4.786	0.053	4.51	0.067
Cortical bone	1850	12.61	0.172	11.93	0.302
Cancellous bone	1080	18.62	0.308	17.79	0.469
Blood	1057	55.48	1.868	54.18	2.283
Muscle	1059	60.73	1.198	57.03	1.840
Grey matter	1035.5	51.80	1.009	47.79	1.525
White matter	1027.4	37.77	0.665	36.58	1.081
Cerebro-spinal fluid	1000	68.29	2.426	67.39	2.842
Sclera/cornea	1151	51.79	1.192	52.69	1.683
Vitreous humour	1000	67.90	1.686	67.19	2.092
Nerve	1112	33.36	0.606	32.09	0.867
Cartilage	1171	40.62	0.828	38.24	1.241
Tongue/thyroid	1059	56.29	1.087	54.07	1.599
Cerebellum	1035.5	49.74	1.066	47.98	1.441
Oesophagus	1126	40.33	0.818	37.07	1.153

The antenna is located vertically beside the head in the frontal plane containing both ears (figure 1(a)) with the dipole feed point in front of the ear at different distances (1–5 cm) from the inner part of the pinna, which is included in the calculations with all three models. The SAR values inside the eye have been obtained, for all frequencies and head sizes, considering a worst case situation in which the antenna is located vertically in the sagittal plane crossing the centre of the eye (figure 1(b)), with the dipole feed point in front of the eye at a distance of 2 cm.

3. Results

We have made SAR calculations, using the XFDTD program, at frequencies of 900 and 1800 MHz, and we have obtained the results shown in tables 2 and 3, respectively, for

Table 2. Local peak SAR, maximum 1 g averaged SAR, maximum 10 g averaged SAR and whole-head averaged SAR in the head. Distance antenna–ear: 2.2 cm. Frequency: 900 MHz. Radiated power: 0.25 W.

	Peak SAR (W kg^{-1})	Max $SAR_{1\,g}$ (W kg^{-1})	Max $SAR_{10\,g}$ (W kg^{-1})	SAR_{wh} (W kg^{-1})
Adult	4.21	2.35	1.44	0.02
88%	3.84	2.06	1.32	0.03
78%	3.36	1.72	1.20	0.04

Table 3. Local peak SAR, maximum 1 g averaged SAR, maximum 10 g averaged SAR and whole-head averaged SAR in the head. Distance antenna–ear: 2.2 cm. Frequency 1800 MHz. Radiated power: 0.125 W.

	Peak SAR (W kg^{-1})	Max $SAR_{1\,g}$ (W kg^{-1})	Max $SAR_{10\,g}$ (W kg^{-1})	SAR_{wh} (W kg^{-1})
Adult	4.56	2.74	1.45	0.008
88%	4.63	2.76	1.43	0.011
78%	4.93	2.71	1.35	0.015

local peak SAR, maximum $SAR_{1\,g}$, maximum 10 g averaged SAR ($SAR_{10\,g}$) and whole-head averaged SAR (SAR_{wh}), including the pinna in the averaging volume, for an antenna–head distance of 2.2 cm, measured from the inner part of the pinna. The maximum SAR values are located on the surface of the head, in the skin tissue layers of the lower part of the pinna.

At 900 MHz, we can observe a trend of decreasing for the local peak, $SAR_{1\,g}$ and $SAR_{10\,g}$ with the scaling down of the head. We also see that there are not many differences in the value of the $SAR_{10\,g}$ for both used frequencies.

On the other hand, we can see that SAR_{wh} increases with the downsizing of the head model. Moreover, a higher SAR_{wh} is observed for the lower frequency while higher superficial (local peak) absorption is obtained at 1800 MHz. This ratifies that field penetration is higher at 900 MHz, as expected. In this case, the lower frequency has twice the radiated power of the higher frequency, but similar qualitative results are obtained if the same radiated power is used for both frequencies.

To study any difference in the energy absorption inside the brain depending on the size of the used head model, the variations of maximum $SAR_{1\,g}$ in the brain as a function of the antenna–head distance have been represented in figure 2 for the full-size model and the 88% and 78% scaled models at the frequencies of 900 MHz (figure 2(a)) and 1800 MHz (figure 2(b)). As can be appreciated in the figure, the absorption inside the brain increases as the size of the models is reduced. This can be due to the important fact that the thickness of the skull and other tissues decreases with the scaling down. The same effect is observed at 1800 MHz. However, when the antenna–head distance becomes greater than 4 cm, in this example, there is almost no difference between the absorption in brain tissues, in the three used models.

The $SAR_{10\,g}$ distribution inside adults and children (88% and 78% models) at 900 MHz in the horizontal plane containing the dipole feed point is depicted in figure 3. The colour scale has been normalized, so the same colour represents the same SAR value in all plots. Their sizes are equal because a greater zoom factor has been used for the smaller models to better appreciate the differences in the absorption. As we have reduced the cell size for the scaling, the antenna–head distance enlarges in terms of cells as the model is reduced, as can be appreciated in the plots, to maintain the same absolute distance in all three cases. We can see

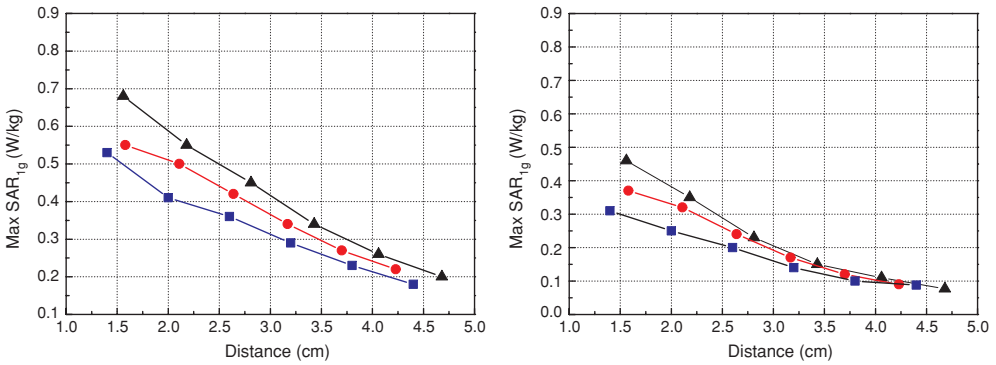

Figure 2. $SAR_{1\,g}$ in brain as a function of antenna–head distance. Comparison between the models for adult (square), 88% (circle) and 78% (triangle) scaled children models. (a) Frequency: 900 MHz. Radiated power: 0.25 W. (b) Frequency: 1800 MHz. Radiated power: 0.125 W.

Table 4. Local peak SAR, maximum 1 g averaged SAR, maximum 10 g averaged SAR, whole-head averaged SAR in the head and maximum 1 g averaged SAR in eye tissues. Distance antenna–eye: 2 cm. Frequency: 900 MHz. Radiated power: 0.25 W.

	Peak SAR (W kg^{-1})	Max $SAR_{1\,g}$ (W kg^{-1})	Max $SAR_{10\,g}$ (W kg^{-1})	SAR_{wh} (W kg^{-1})	Max $SAR_{1\,g}$ (eye) (W kg^{-1})
Adult	4.14	2.34	1.45	0.019	2.03
88%	4.11	2.26	1.32	0.026	2.02
78%	4.01	2.37	1.30	0.037	2.08

clearly that under these circumstances a higher percentage of energy is absorbed by the brain in the reduced model as compared to the adult model, and contour plots of the same value are deeper (in terms of cells) in the smaller models.

The $SAR_{10\,g}$ distribution inside adults and children (88% and 78% scaled models) at 1800 MHz in the horizontal plane defined above is shown in figure 4. It is clear that field penetration into the head is small at this frequency and then, obviously, SAR variation with the size of the head is very slight, the $SAR_{10\,g}$ in brain tissue being 9 dB under the maximum for the 78% scaled model.

In order to analyse possible differences in SAR between the three used models due to the consideration of anatomical details in the simulation, an antenna–head configuration has been studied with the antenna located 2 cm in front of the eye, as a worst case situation. The calculated results for local peak SAR, maximum $SAR_{1\,g}$, maximum $SAR_{10\,g}$ and SAR_{wh} at the frequencies of 900 and 1800 MHz are shown in tables 4 and 5, respectively. Moreover, the maximum SAR inside the eye, as a critical outer organ, has been explicitly set out in the tables. In this case, because of the small size and weight of the eye, only $SAR_{1\,g}$ has been computed. For each frequency, the values of the maximum $SAR_{1\,g}$ in the eye are almost the same in the three models and, even in such a worst case like the one analysed, they are only slightly over the ANSI/IEEE standard limit (1.6 W kg^{-1}).

As an example of SAR distribution obtained with this geometrical configuration, comparison between the $SAR_{1\,g}$ contour plots for the adult model and the 78% scaled model at 900 MHz in the horizontal plane containing the dipole feed point is shown in figure 5. As can be seen, a very similar $SAR_{1\,g}$ distribution in the eye is obtained with both models although the

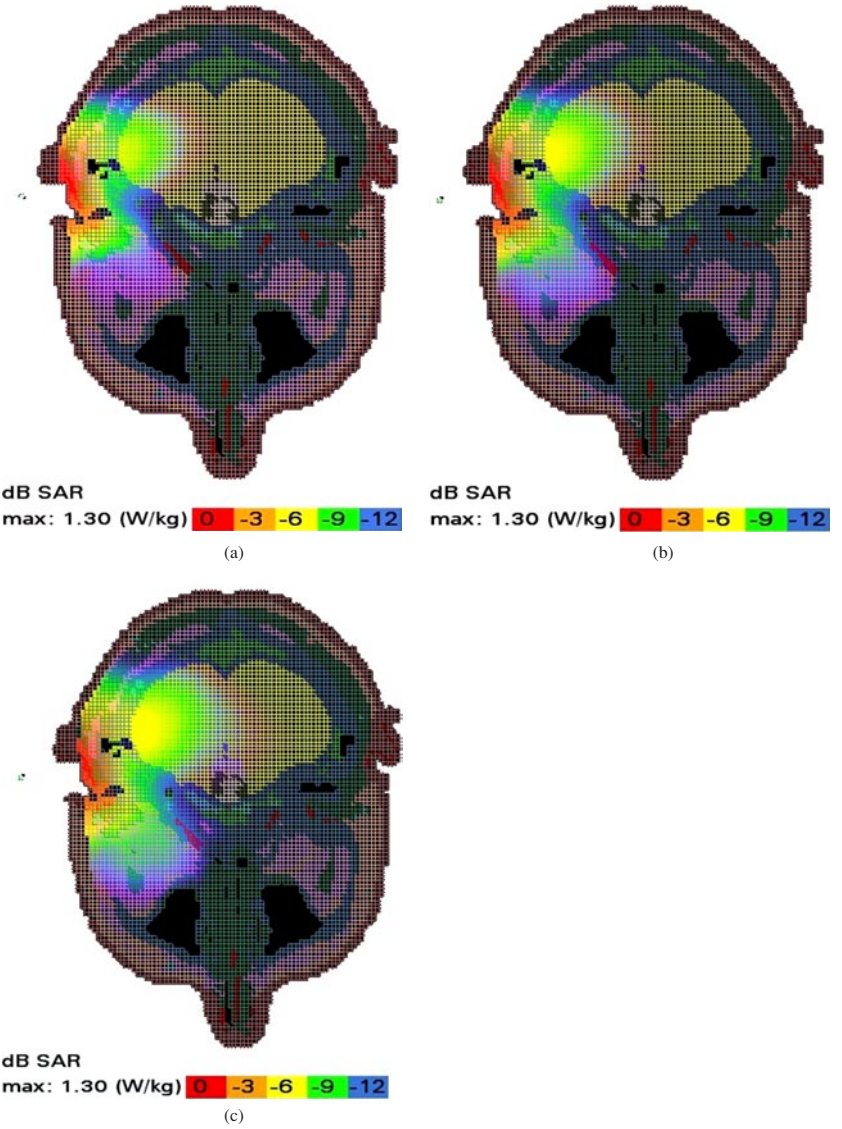

Figure 3. $SAR_{10\,g}$ distribution in a realistic human head model. (a) Adult. (b) Child 88% scaled. (c) Child 78% scaled. Radiated power: 0.25 W. Frequency: 900 MHz. Antenna–head distance: 2.2 cm.

frequency is 900 MHz, that is, the energy absorption takes place in the outer tissue layers for both adult and children models, due to the dielectric characteristics of the eye and surrounding tissues.

4. Conclusions

In this work, SAR deposition in different sizes of human head has been analysed to study the possible differences in energy absorption between adults and children when they are exposed

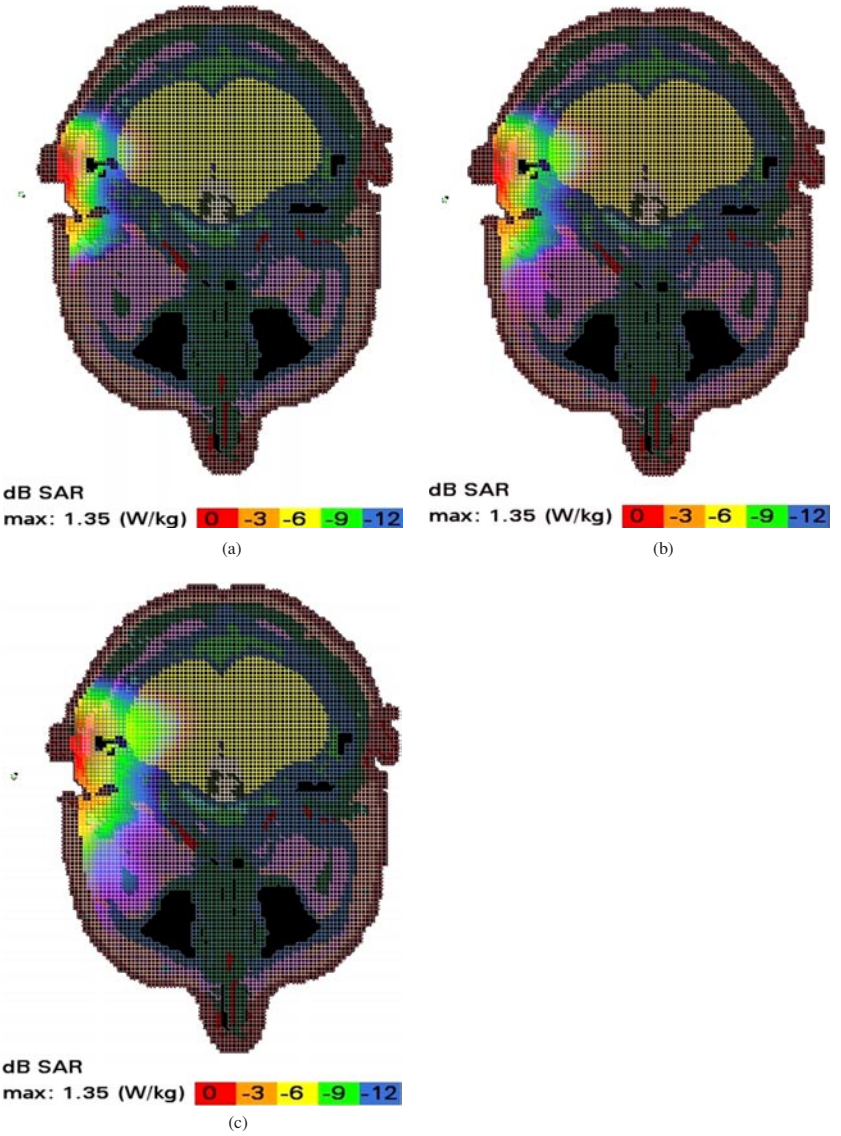

Figure 4. $SAR_{10\,g}$ distribution in a realistic human head model. (a) Adult. (b) Child 88% scaled. (c) Child 78% scaled. Radiated power: 0.125 W. Frequency: 1800 MHz. Antenna–head distance: 2.2 cm.

to the electromagnetic radiation from a mobile phone. Moreover, the study of the absorption inside the eye, as a critical organ, has been included. All the simulations have been made at two frequencies, 900 and 1800 MHz, for comparison.

Peak SAR and $SAR_{1\,g}$ show strong variations between neighbour cells of different tissues with different dielectric characteristics; this behaviour can explain the different results obtained by several authors relating to maximum SAR, which is always found in the surface of the head model, where different tissues are modelled in a small region that is highly affected by the scaling in size. Setting the radiated power to values currently used (0.250 W for

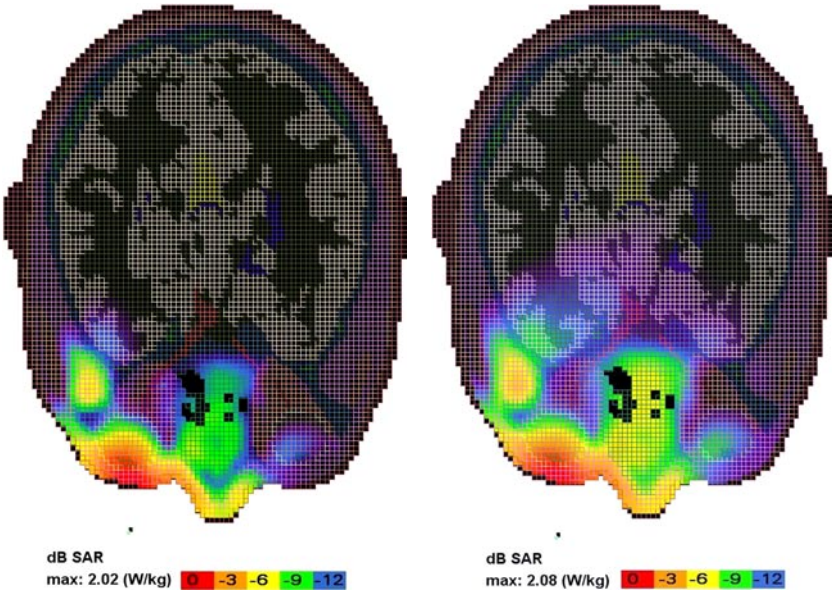

(a) (b)

Figure 5. $SAR_{1\,g}$ distribution in the eye in a realistic model. Comparison between (a) adult and (b) child (78% scaled model). Radiated power: 0.25 W. Frequency 900 MHz.

Table 5. Local peak SAR, maximum 1 g averaged SAR, maximum 10 g averaged SAR, whole-head averaged SAR in the head and maximum 1 g averaged SAR in eye tissues. Distance antenna–eye: 2 cm. Frequency 1800 MHz. Radiated power: 0.125 W.

	Peak SAR (W kg^{-1})	Max $SAR_{1\,g}$ (W kg^{-1})	Max $SAR_{10\,g}$ (W kg^{-1})	SAR_{wh} (W kg^{-1})	Max $SAR_{1\,g}$ (eye) (W kg^{-1})
Adult	5.25	2.85	1.44	0.007	1.76
88%	5.24	2.61	1.33	0.010	1.70
78%	4.57	2.12	1.21	0.015	1.63

900 MHz and 0.125 W for 1800 MHz), quite similar values of maximum $SAR_{10\,g}$ are obtained for models of different sizes. However, we observe an increase in the SAR_{wh} value with the downsizing of the model, as expected. Our findings completely agree with the results of Lee *et al* (2002).

Nevertheless, differences in SAR inside the brain have been found at 900 and 1800 MHz depending on the size of the model. Higher SAR in the brains of children can be expected depending on whether the thickness of their skulls and surrounding tissues actually depends on age.

When the $SAR_{1\,g}$ in the eye is studied, a very similar distribution for the full size and the scaled models has been obtained, the penetration depth being quite similar too. In this case, where the maximum $SAR_{1\,g}$ is located near the eye, it has been shown that the ANSI/IEEE standard limit (1.6 W kg^{-1} for $SAR_{1\,g}$) can be exceeded if the antenna–eye distance is about 2 cm (or lower), a quite unpractical situation.

The SAR distributions analysed show that 10 g averaged SAR values are always below the European standard limit (2 W kg^{-1}) for the supposed exposure conditions.

Acknowledgments

This work has been supported by the PN I + D + I of the Spanish Ministry of Science and Technology, project TIC 2000-0698 and PROFIT 2000-2003, FIT-070000-2002-135. We would also like to thank the European Social Fund for the I3P program work contract for the author M Anguiano in the CSIC.

References

American National Standards Institute (ANSI)/IEEE 1992 Safety levels with respect to human exposure to radiofrequency electromagnetic fields. 3 KHz to 300 GHz *ANSI/IEEE Std* C.95.1 (New York: The Institute of Electrical and Electronics Engineers (IEEE) Inc.)

COST (European Cooperation on Science and Technology) 2002 *Watchdog Report* COST 281 (http://www.cost281.org/activities/watchdog-report2002.pdf)

Dimbylow P J 1993 FDTD calculations of the SAR for a dipole closely coupled to the head at 900 MHz and 1.9 GHz *Phys. Med. Biol.* **38** 361–8

European Commission 1999 Council recommendation of 12 July 1999 on the limitation of exposure of the general public to electromagnetic fields (0 Hz to 300 GHz) *Official Journal of the European Communities* **L199** 59 (1999/519/EC)

Gabriel C and Gabriel S 1996 Compilation of the dielectric properties of body tissues at RF and microwave frequencies *Technical Report* AL/OE-TR-1996-0037 (London: Physics Department, King's College)

Gandhi O P and Kang G 2001 Effect of the head size on SAR for mobile telephones at 835 and 1900 MHz *24th Annual Meeting of the Bioelectromagnetics Society Abstract Book (St Paul, MN)* p 52

Gandhi O P, Lazzy G and Furse C M 1996 Electromagnetic absorption in the human head and neck for mobile telephones at 835 and 1900 MHz *IEEE Trans. Microw. Theory Tech.* **44** 1884–97

Hombach V, Meier K, Burkhardt M, Kühn E and Kuster N 1996 The dependence of EM energy absorption upon human head modeling at 900 MHz *IEEE Trans. Microw. Theory Tech.* **44** 1865–73

Independent Expert Group on Mobile Phones (IEGMP) 2000 *The Stewart Report* http://www.iegmp.org.uk/

Lee A, Choi H and Pack J 2002 Human head size and SAR characteristics for handset exposure *ETRI J.* **24** 176–9

Martínez-Búrdalo M, Nonídez L, Martín A and Villar R 2001 FDTD analysis of the maximum SAR when operating a mobile phone near a human eye and a Wall microwave *Opt. Technol. Lett.* **28** 83–5

National Institute of Standards and Technology (NIST) 1977 *Anthropometric Data of Children* http://www.itl.nist.gov/iaui/ovrt/projects/anthrokids/77mINF.htm

Okoniewski M and Stuchly M 1996 A study of the handset antennas and human body interaction *IEEE Trans. Microw. Theory Tech.* **15** 1855–64

Peyman A, Rezazadeh A and Gabriel C 2001 Changes in the dielectric properties of rat tissue as a function of age at microwave frequencies *Phys. Med. Biol.* **46** 1617–29

Schöborn F, Burkhardt M and Kuster N 1998 Differences in energy absorption between heads of adults and children in the near field of sources *Health Phys.* **74** 160–8

Shlager K L and Schneider J B 1995 A selective survey of the finite-difference time-domain literature *IEEE Antennas Propag. Mag.* **37** 39–56

Taflove A and Hagness S C 2000 *Computational Electrodinamics: The Finite-Difference Time-Domain Method in Electromagnetics* (Norwood, MA: Artech House)

Wang J and Fujiwara O 2002 Comparison and evaluation of local peak SAR in realistic human head models of adult and children for mobile phones *URSI General Assembly CD Abstracts KB.O.6* (also at http://hawk.iszf.irk.ru/URSI2002/GAabstracts/papers/p0129.pdf)

Wang J and Fujiwara O 2003 Comparison and evaluation of electromagnetic absorption characteristics in realistic human head models of adult and children for 900-MHz mobile telephones *IEEE Trans. Microw. Theory Tech.* **51** 966–71